

Auger spectrum of the noble gases. II. Argon*

Eugene J. McGuire

Sandia Laboratories, Albuquerque, New Mexico 87115

(Received 20 January 1975)

Theory and experiment are compared for the $L_{23}MM$ principal and satellite spectra of argon. For the principal spectrum it is shown that theory and experiment are in excellent agreement if the doublet conventionally assigned to $L_{23}M_1M_1$ is reassigned to $L_{23}M_1M_{23}$ (1P). It is hypothesized that the splitting of the 1P term is due to configuration interaction with the $(3p)^32D(3d)^1P$ term of Ar^{+2} . The reassignments enable us to locate, tentatively, several unknown singlet levels in Ar^{+2} . An examination of the satellite spectrum confirms Mehlhorn's assignment of the terms in the $Ar^{+2}(2p)^5(3s)^2(3p)^5$ configuration. The calculated satellite spectra agree with experiment in spectral shape (the location of peaks) and agree to a factor of 2 in individual satellite peak intensity. The satellite calculations support Mehlhorn's conclusion that theory considerably overestimates the $L_1L_{23}M_1$ Auger transition rate.

I. INTRODUCTION

An earlier paper¹ in this sequence treated the $M_{4,5}NN$ principal and satellite Auger spectrum of krypton. Krypton was chosen to initiate the sequence because there was a serious difference between calculations and measurement for the $[4s]^2$ vacancy configuration energy level, and because the satellite spectrum was expected to be relatively simple. The serious difference occurred because there are two doublets in the Kr $M_{4,5}NN$ Auger spectrum, either of which could be identified with the $M_{4,5}N_1N_1$ transition. If the larger of the doublets were so identified, then the calculated and measured energy of the Auger electron in the $M_{4,5}N_1N_1$ transition would differ by about 10 eV. In addition, the calculated value of the $M_{4,5}N_1N_{2,3}$ (1P_1) intensity was significantly larger than the measured value. It was shown in Ref. 1 that these differences between calculation and experiment could be resolved if the smaller doublet was identified with the $M_{4,5}N_1N_1$ transition, and the larger doublet was associated with the $M_{4,5}N_1N_{2,3}$ (1P_1) transition, but separated in energy by configuration interaction. It will be shown that a similar situation occurs in Ar.

In Ref. 1 it was shown that there was good agreement between the calculated and measured satellite spectra when the energy levels in initial and final states were known experimentally or were calculable by simple atomic structure techniques; i.e., agreement was poor when configuration interaction effects were important but not accounted for. The analysis for Kr was simplified because the dominant mechanism in producing the initial state in the satellite spectra was the $[3p] \rightarrow [3d][4p]$ Coster-Kronig transition. In Ar, calculations indicate the initial state in the satellite spectra arises from both the $[2s] \rightarrow [2p][3s]$ and $[2s] \rightarrow$

$[2p][3p]$ Coster-Kronig transitions. One then expects overlapping spectra from $[2p][3s] \rightarrow [3s][3p]^2$ and $[2p][3p] \rightarrow [3p]^3$. Mehlhorn's analysis of his measurements² on the $L_1-L_{23}M$ Auger transition indicate the $L_1-L_{23}M_1$ transition rate is much smaller than the calculated value. This would lead to a simple satellite spectrum. However, the $L_1-L_{23}M_1$ transition occurs at about 30 eV where the background is large and rapidly rising. Mehlhorn finds the L_1 width to be 1.84 ± 0.2 eV. Theoretical values^{3,4} are in the 2.7–2.9 eV range. The difference between theory and experiment is entirely due to the $L_1-L_{23}M_1$ value.³ Clearly an analysis of the satellite spectra should illuminate this question. The procedure we use is similar to that used in optical spectroscopy, i.e., to locate a level by observing transitions in which the level is both a final and an initial state. However, as in optical spectroscopy, one must identify the transitions arising from different ionization states. This we do in the next section.

As was the case with Kr, the analysis of the Auger spectrum in Ar is hindered because so few of the required energy levels have been observed in the optical and soft-x-ray spectroscopy.⁵ I have suggested elsewhere⁶ that population inversions produced by Auger transitions can lead to amplified spontaneous emission in the soft-x-ray region. To examine specific cases requires knowledge of just these unknown energy levels. The analysis of the principal and satellite Auger spectra can provide some of the missing information.

II. THE $L_{23}-MM$ SPECTRUM OF Ar

In Figs. 1 and 2 we show recent high-resolution measurements of Werme *et al.*⁷ of the $L_{23}-MM$ spectrum of Ar. Werme *et al.*⁷ list energies and intensities for the 82 identified lines. Earlier,

Mehlhorn and Stalherm⁸ measured this spectrum with poorer resolution. The data on the principal spectrum are shown in Table I where we have normalized the data of Mehlhorn and Stalherm⁸ so that their $L_{2,3}-M_{23}M_{23}$ (1S) intensity agrees with that of Werme *et al.*⁷ The values calculated by Rubenstein⁴ and McGuire³ are normalized so that the

summed L_2-MM (L_3-MM) intensity equals the summed L_2-MM (L_3-MM) intensity of Werme *et al.* Werme *et al.*⁷ measure an L_2 or L_3 level width of 0.17 eV, in excellent agreement with the calculations of Ref. 3 but higher than those of Ref. 4. Two major disagreements between theory and experiment are apparent. Theory overestimates the

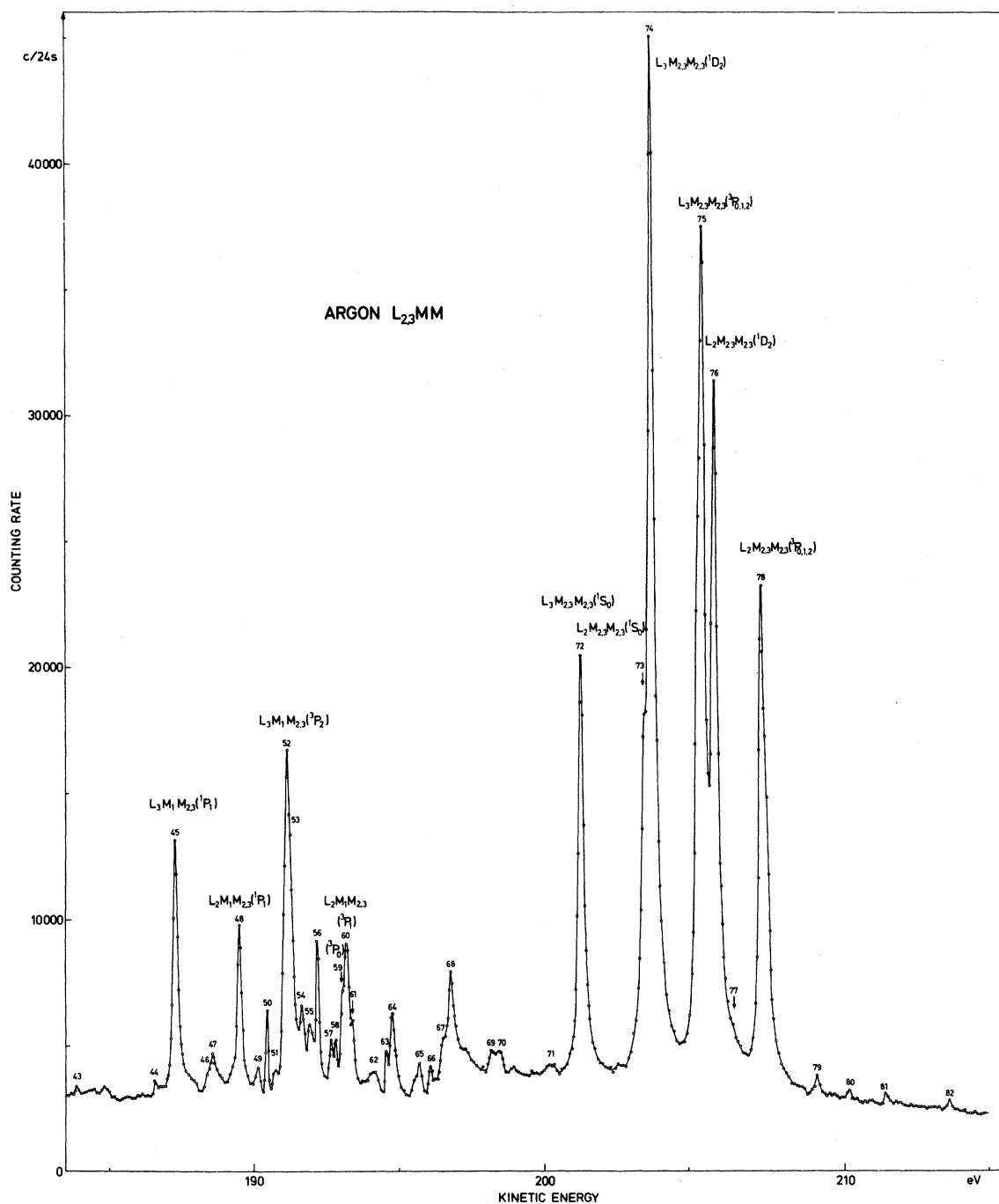


FIG. 1. Measurements of Werme *et al.* (Ref. 7) of the Ar L_{23} MM Auger spectra from 185 to 215 eV.

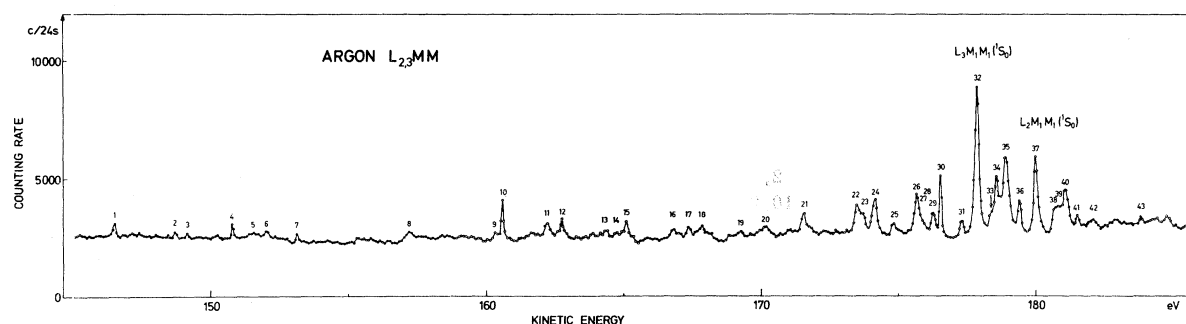


FIG. 2. Measurements of Werme *et al.* (Ref. 7) of the Ar $L_{23}MM$ Auger spectra from 140 to 185 eV.

$L_{2,3}-M_1M_{2,3}({}^1P)$ intensity and underestimates the $L_{2,3}-M_1M_1({}^1S)$ intensity.

An explanation for the discrepancy is that the $L_{2,3}-M_1M_1({}^1S)$ doublet has been misidentified. Lines 37 and 32 are the strongest set of lines, separated by 2.16 eV, the L_2-L_3 splitting, in the spectral region where one expects the $L_{2,3}-M_1M_1$ doublet to be located. However, this is not sufficient reason to assign peaks 37 and 32 to the $L_{23}-M_1M_1$ doublet. In Table II we list nine doublets with approximately the L_2-L_3 splitting, $\Delta E = 2.16$ eV. Lines 34 and 32 are listed twice. Lines 38 and 39 are within 0.1 eV, and either could form a doublet with line 34. The doublet *f* has the wrong relative intensity, but doublet *e* could have intensity 18, 29 and doublet *f* intensity 5, 11 as they share level 32. The absolute energy of the final-state term in the Auger transition is obtained by subtracting ΔE from the energy position of the high line, arising from L_2 decay, and subtracting the resultant from the energy of the $L_3M_1M_{2,3}({}^3P_2)$. The difference is added to the energy position of the $M_1M_{2,3}({}^3P_2)$ level as de-

termined from Moore's tables.⁵ In Fig. 3 we show the calculated and observed⁵ positions of $(3p)^4$ and $(3s)(3p)^5$ levels. For the $(3p)^4$ configuration the calculated 3P position was equated to the observed position.⁵ The calculated term splittings were obtained from atomic structure expressions⁹ and radial integrals in Mann's tables.¹⁰ Agreement between calculation and experiment is good, indicating no significant configuration interaction. For the $(3s)(3p)^5$ configuration, we equated the calculated and observed position of the 3P . There is then a significant difference between calculation and experiment for the 1P position. This indicates strong configuration interaction. It is to this configuration interaction that I attribute the difference in intensities between theory and experiment shown in Table I.

Also shown in Fig. 3 are the observed position⁵ of other 3P levels in Ar III. Unfortunately, Moore's Tables⁵ contain no information on highly excited singlet terms in Ar III. While such information would be extremely useful, we can interpret the

TABLE I. Comparison of conventionally assigned experimental $L_{23}MM$ Auger peaks with calculated values for argon.

Transition	Line number	Measured intensity		Calculated intensity	
		Ref. 7	Ref. 2	Ref. 3	Ref. 4
$L_2M_1M_1({}^1S)$	37	18	31.5	6.1	6.7
$L_2M_1M_{2,3}({}^3P)$	59, 60	37	59	45.5	57.8
$({}^1P)$	48	32	37	52.4	64.3
$L_2M_{23}({}^3P)$	78	139	176	151	170
$({}^1D)$	76	183	213	178	143
$({}^1S)$	73	55	55	41.2	32.7
$L_3M_1M_1({}^1S)$	32	34	59	10.2	11.8
$L_3M_1M_{2,3}({}^3P)$	52	87	91	80.4	102
$({}^1P)$	45	53	65.6	92.5	114
$L_3M_{23}({}^3P)$	75	272	343	266	300
$({}^1D)$	74	270	377	314	252
$({}^1S)$	72	100	100	72.8	57.7
$\Gamma_{L_{2,3}}$ (eV)		0.17		0.167	0.100

TABLE II. Doublets in the $L_{23}MM$ argon Auger spectrum with spacing of 2.16 eV.

Doublet	Lines	Line intensity	Position of high line (ev)	ΔE (eV)	Absolute energy of low level (eV)
<i>a</i>	41, 36	2, 6	181.58	2.10	25.75
<i>b</i>	40, 35	10, 21	181.14	2.17	26.26
<i>c</i>	39, 34	5, 12	180.88	2.22	26.47
<i>d</i>	38, 34	5, 12	180.78	2.12	26.57
<i>e</i>	37, 32	18, 34	180.06	2.15	27.32
<i>f</i>	32, 26	34, 11	177.91	2.15	29.47
<i>g</i>	29, 24	6, 11	176.32	2.10	31.01
<i>h</i>	23, 21	5, 7	173.81	2.21	33.63
<i>i</i>	13, 11	1, 4	164.42	2.16	42.97

doublet structures (*a* to *i*) without it. The absolute energies of final state terms in the Auger transitions determined in Table II are also shown in Fig. 3. The terms deduced from the doublets *a* and either *c* or *d* can be assigned to the triplet terms $(3p)^3 2P(4s)^3 P$ and $(3p)^3 2P(3d)^3 P$, respectively. This assignment was made by Werme *et al.*⁷ The surprising feature is that, if one interprets these doublets as arising from configuration interaction with $(3s)(3p)^5 3P$, there is no configuration interaction with $(3p)^3 2D(3d)^3 P^0$. Next I assign *b* and *c* or *d* to $(3p)^3 2P(4s)^1 P^0$ or $(3p)^3 2P(3d)^1 P^0$, while I assign *e* to $(3p)^3 2D(3d)^1 P^0$. This last assignment of term *e* indicates that $(3p)^3 2D(3d)^1 P$ is shifted upward

in energy from its expected position [near $(3p)^3 2D(3d)^3 P^0$] by about the same amount (≈ 3 eV) as $(3s)(3p)^5 1P^0$ is shifted downward. It is these levels that have the large configuration interaction, and both will have a large Auger transition rate. The term *e* arises from the doublet that was assigned^{7,8} to $L_{2,3}-M_1M_1$. The question then is where is $L_{2,3}-M_1M_1$? Near level *f* in Fig. 3 is shown the high- and low-energy triplet terms arising from the even parity $(3p)^3 2P(4p)$ configuration. We assign level *f* to the $(3p)^3 2P(4p)^1 S$ term. It is expected that this term will have some configuration interaction with the $(3s)^0(3p)^6 1S$ term. This latter term is assigned to level *g*. Levels *h* and *i* are assigned to the $(3p)^3 2D(4d)^1 P^0$ and $(3p)^3 2D(5d)^1 P^0$ terms, though this assignment is tentative. Thus, we have assigned the nine levels associated with the doublets.

The effect of this reassignment on the comparison between theory and experiment is shown in Table III. The experimental data of Werme *et al.*⁷ is listed, and the two theoretical calculations,^{3,4} normalized to Werme's group intensity. The calculated individual term intensities are now in better agreement with experiment. The remarkable feature is the exceptionally good agreement of Rubenstein's configuration intensities with the reassigned experimental values. The measured $L_{2,3}-M_1M_1$ intensity is twice the calculated value. This disagreement could be removed if we reassigned or eliminated level *f* in Fig. 3. However, if we retain the identification of level *g* as $(3s)^0(3p)^6 1S$, its proximity to $(3s)^2(3p)^3 2P(4p)^1 S$ should cause some configuration interaction.

The level assignments made in Fig. 3 are based on two considerations; first, a consistent and reasonable assignment of all the observed doublets with the L_2-L_3 splitting, and, second, the belief that the calculations are correct. As a consequence, we are able to locate several unknown levels in the Ar III spectrum. One would like some other experimental confirmation of these assign-

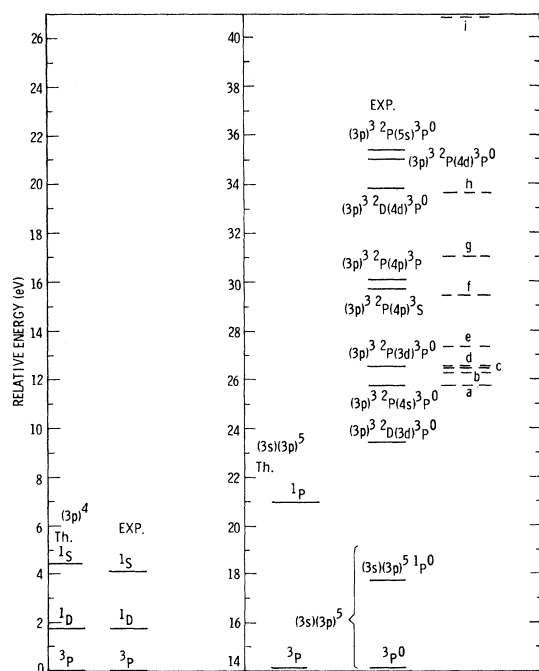
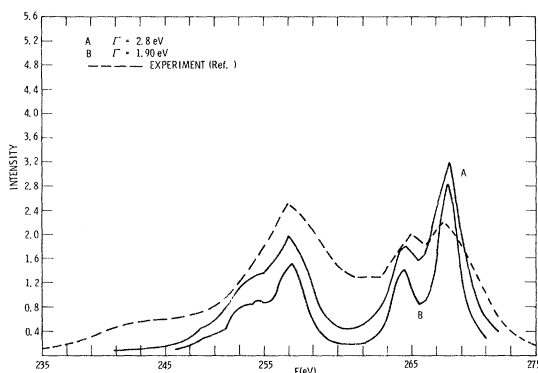
FIG. 3. Energy levels for low-lying terms in Ar^{+2} .

TABLE III. Comparison of the reassigned experimental $L_{23}MM$ Auger spectrum with calculated values.

Transition	Line number	Relative intensity		
		Ref. 7	Ref. 3	Ref. 4
$L_2M_1M_1(^1S)$	32	5	6.5	7.1
	29	6		
$L_2M_1M_{23}(^3P)$	59, 60	37		
	41	2	48.3	61.3
$L_2M_1M_{23}(^1P)$	39 or 38	5		
	48	32	104	129
	40	10		
	39 or 38	5	55.5	68.2
	37	18		
	23	5		
	13	1		
$L_2M_{23}M_{23}(^3P)$	78	139	160.0	181.0
(^1D)	76	183	393	368
(^1S)	73	55	43.7	34.7
$L_3M_1M_1(^1S)$	26	11	11.4	12.8
	24	11		
$L_3M_1M_{23}(^3P)$	52	87		
	36	6	85.4	108.0
	34	6		
$L_3M_1M_{23}(^1P)$	45	53	184	229
	35	21		
	34	6	98.2	121.0
	32	34		
	21	7		
	11	4		
$L_3M_{23}M_{23}(^3P)$	75	272	282.0	318.0
(^1D)	74	270	693	647
(^1S)	72	100	77.3	61.3

ments. Mehlhorn² has measured the weak L_1 - MM Auger spectrum of Ar. In comparing his measurements with calculated intensities, a difficulty occurs in that, with the assignment of level e to the $(3s)^0(3p)^6^1S$ term, the calculations do not span the energy width of the observations. This situation is improved with our new assignments. The ener-

gies are taken from Fig. 3. Our (Rubenstein's) relative intensities for the $L_1M_1M_1(^1P)$, $L_1M_1M_{23}(^1P)$, $L_1M_1M_{23}(^3P)$, $L_1M_{23}M_{23}(^1D)$, and $L_1M_{23}M_{23}(^1S)$ transitions are 0.32 (0.42), 0.85 (0.83), 1.00 (1.00), 0.016 (0.008), and 0.080 (0.083), respectively. The two calculations are in reasonable agreement. From the measured relative intensities in Table III we determine configuration interaction mixing parameters. With this information, we calculate the L_1MM Auger spectrum of Ar. The results along with the experimental measurement are shown in Fig. 4, with two values ($\Gamma=2.8$ and $\Gamma=1.9$ eV) for the L_1 level width. With the new level assignments, the calculated width of the L_1 - MM transition complex is approximately equal to the measured value. The two low-energy peaks, at 256 and 265 eV, are approximately equal in intensity as observed, but the high-energy peak at 266.5 eV is then larger than the observed value. The dip between low-energy peaks is larger than the observed dip. The agreement with experiment is not entirely satisfactory, but the new level assignments lead to an improvement in the lower-energy region of the transition complex.

FIG. 4. Comparison of calculated and experimental Ar L_1MM Auger spectra.

III. THE $L_{23}M$ -MMM SATELLITE SPECTRUM OF ARGON

There are two mechanisms which can lead to prominent L_{23} -MM Auger satellite structure in Ar. Carlson and Nestor¹¹ have estimated a probability of 13% for shakeup and shakeoff of a $3p$ electron when a $2p$ electron is ionized in Ar. In Ref. 1 it was concluded that for Kr the satellite data were inconsistent with substantial shakeoff, and with substantial shakeup followed by autoionization of the outer electron prior to the Auger transition. The data were consistent with shakeup, followed by an Auger transition prior to autoionization of the outer electron. A shakeup term of the form $(2p)^5[(3p)^5(4p)^1S]^2P$ can Auger decay into many final-state terms, and it is assumed no transition is sufficiently strong to significantly affect the satellite spectrum. The alternative mechanism is the L_1 - $L_{23}M$ Auger decay. To estimate the overall intensity of the satellite spectrum arising from L_1 - $L_{23}M$ Auger decay, one needs the cross sections for $2s$ and $2p$ ionization by 3-keV electrons. Direct calculations by the author¹² lead to $\sigma_{2p} = 1.2 \times 10^{-18} \text{ cm}^2$. Direct calculations were not done for $2s$ ionization in Ar. However, they were done for $2s$ ionization in Be-Na. The cross section for the different elements could be fitted by an expression of the form¹³

$$\sigma_{2s}(E_{2s})^{2.15} = g(E/E_{2s}),$$

where E_{2s} is the $2s$ ionization energy, E is the incident electron energy, and g is a "universal" function. The departure of the exponent from 2.0 has been experimentally verified for the $2p$ shell by Vrakking and Meyer.¹⁴ Extrapolating this reduced cross section to Ar leads to $\sigma_{2s} = 7.5 \times 10^{-20}$, and $\sigma_{2s}/\sigma_{2p} = 0.063$. This leads to an $L_{2,3}M$ vacancy

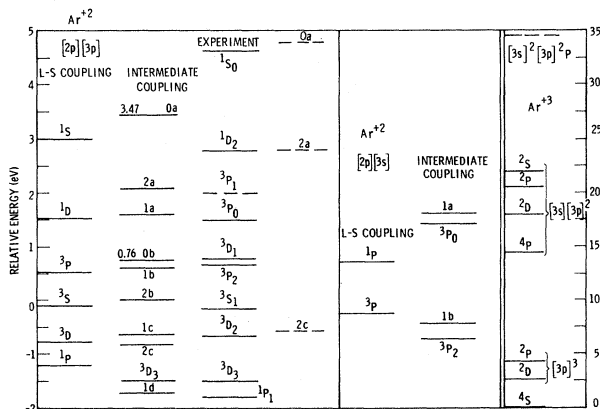


FIG. 5. High-lying terms of Ar^{+2} and low-lying terms of Ar^{+3} . The procedures used to predict the high-lying terms of Ar^{+2} are discussed in the text.

population via L_1 - $L_{23}M$ Auger decay that is roughly half that estimated for shakeup and shakeoff. We will see that 0.063 may be a factor of 2 too large! Using this ratio for σ_{2s}/σ_{2p} will normalize the calculated satellite spectrum to the main spectrum.

When electrostatic splitting and spin-orbit interaction are included, there are 14 terms that are populated by L_1 - $L_{23}M$ Auger transitions. We show the relative positions of these levels in Fig. 5. For the $(2p)^5(3p)^5([2p][3p])$ configuration in Ar^{+2} , Fig. 5 shows the calculated electrostatic term splitting, the additional term splitting due to spin-orbit interaction, and the experimental values of Mehlhorn² obtained by fitting the observed L_1 - $L_{23}M_{23}$ transition complex. We use the notation 1a, 1b, etc., to indicate the highest energy level with $J=1$, the next highest with $J=1$, etc. Mehlhorn retains the L - S coupling notation, designating a level by its predominant component. There are significant differences between the experimental splitting and that calculated in intermediate coupling. However, for interpreting the satellite spectrum, it is the shift of 1D_2 and 1S_0 relative to 3D_3 that is most important. For the $(2p)^5(3s)(3p)^6$ configuration the important levels are 1a and 1b. Our calculations indicate they are split by 2.1 eV, close to the L_2 - L_3 splitting! Satellites arising from these two levels could be included in the listing of doublets in Table II! In the last section of Fig. 5 we list low-lying levels in Ar^{+3} . We also include the $(3s)^0(3p)^5^2P$ level which we will locate from Figs. 1 and 2.

The relative importance of terms in the $L_{23}M$ configurations for the Auger spectrum can be estimated from Table IV. Here we list the initial $L_{23}M$ terms, their relative energy positions as

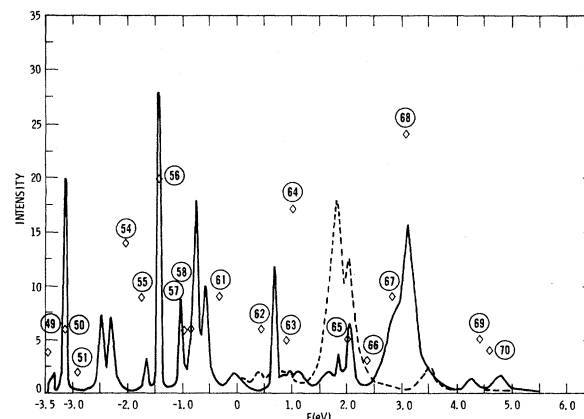


FIG. 6. Calculated and measured $L_{23}M_{23}-(M_{23})^3$ Auger satellite spectrum. The dashed curve is generated using the intermediate coupling energy values for 2a and 0a in Fig. 5, while the solid curve arises from Mehlhorn's assignment of these levels.

calculated in intermediate coupling (for $0a$ and $2a$ we show adjusted positions in parentheses), their initial populations, the transition rates to various final states (in $10^{-4}/\text{atu}$; $1 \text{ atu} = 2.42 \times 10^{-17} \text{ sec}$), and the widths associated with each of the initial terms. We fold the transitions, taken as Lorentzians, with a rectangular window of 0.075 eV to account for the resolution of Werme *et al.*⁷ Transition rates used in the calculations are given elsewhere.¹⁵

The level 3D_3 has a large initial population and a small width. It decays primarily to four final states $[3p]^3^2D$, $[3p]^3^2P$, $[3s][3p]^2^2D$, and $[3s]^2[3p]^2P$. The energy difference between $[3p]^3^2D$ and $[3p]^3^2P$ is 1.71 eV and between $[3p]^2^2D$ and $[3s][3p]^2^2D$ is 15.5 eV . The energy difference between peaks 56 and 50, and 56 and 30 in Figs. 1 and 2 are 1.71 eV and 15.55 eV , respectively. Peaks 56, 50, and 30 are narrow, of roughly the appropriate intensity, and at the appropriate energy difference. Peak 10 is narrow and has roughly the appropriate intensity, and so allows us to identify it as the $(2p)^5(3p)^5^3D_3 - (3s)^0(3p)^5^3P$ transition. Thus, we locate the $[3s]^2[3p]^2P$ term in Fig. 5.

Having established an absolute energy scale via transitions arising from $[2p][3p]^3D_3$, we calculated the satellite spectrum with the term splitting cal-

culated in intermediate coupling. In Fig. 6 we show the calculated $L_{23}M_{23}-(M_{23})^3$ spectrum as a solid curve, and as a dashed curve. There is no experimental peak corresponding to the large dashed structure at 1.80 eV in Fig. 6. We then repeated the calculation shifting the $2a$ term upwards by 0.7 eV and the $0a$ term by 1.3 eV , without changing the intermediate coupling mixing parameters. The result is the solid curve in Fig. 6. The $0a$ level in Fig. 5 is then 0.14 eV higher than the position estimated for it by Mehlhorn.² Shifting of these two levels brings peaks 65, 67, and 68 into reasonable agreement with the calculation. Two aspects of Mehlhorn's identification² have been verified. First, that the observed $L_1-L_{23}M_{23}$ transition complex contains only ten peaks. An alternative to Mehlhorn's resolution of the complex is that it is composed of ten peaks unshifted from their intermediate coupling values, plus some additional unknown structure. However, we have shown that the unshifted intermediate coupling terms leads to a large peak where the data indicate no peak. Second, Mehlhorn's estimated shifts of levels $0a$ and $2a$ from 3D_3 lead to good agreement with the satellite data.

There are disagreements between the calculation and experiment in Fig. 6. The value of intensity for peak 50 is much smaller than the calculated

TABLE IV. Populations, relative energies, and transition rates for the $L_{23}M-MMM$ Auger satellite spectra.

Initial state term			Final state term and energy									
Relative energy (eV)	Intensity		4S (0.00)	$[3p]^3$ 2D (2.62)	2P (4.33)	4P (14.6)	$[3s][3p]^2$ 2D (18.1)	2P (20.6)	2S (22.0)	$[3p][3s]^2$ 2P (34.5)	A_{tot} ($10^{-4}/\text{atu}$)	Γ (eV)
[2p][3p]												
1d	-1.71	0.78	0.50	2.01	1.26	0.26	0.078	2.06	0.043	0.79	7.00	0.019
3D_3	-1.49	6.95	0.0	1.13	0.805	0.001	0.710	0.008	0.001	0.79	3.45	0.0094
2c	-0.82	4.50	1.42	8.50	3.90	0.735	2.59	0.99	0.0	0.79	18.9	0.0513
1c	-0.63	5.04	5.83	9.68	6.60	3.00	0.063	4.00	0.45	0.79	29.4	0.0798
2b	0.02	0.62	17.1	37.4	22.2	8.82	3.55	11.7	0.0	0.79	101.6	0.276
1b	0.62	2.85	0.042	1.14	0.79	0.023	0.55	0.35	0.052	0.79	3.73	0.0101
0b	0.78	2.00	17.0	28.0	29.80	8.77	0.0	11.7	4.08	0.79	100.2	0.272
1a	1.604	1.84	14.2	23.6	15.9	7.35	0.034	9.85	0.161	0.79	72.0	0.196
2a	2.075 (2.78)	3.35	2.08	50.3	18.0	1.07	18.0	1.43	0.0	0.79	91.7	0.250
0a	3.47 (4.76)	9.40	3.62	5.94	55.0	1.86	0.0	2.48	19.2	0.79	89.0	0.242
[2p][3s]												
3P_2	-0.72	0.12 (0.06)				20.6	19.5	2.58	5.35	8.04	56.1	0.153
1b	-0.42	17.1 (8.6)				11.5	19.5	11.6	5.35	5.09	53.1	0.144
3P_0	1.44	0.024 (0.012)				20.6	19.5	2.58	5.35	8.04	56.1	0.153
1a	2.63	21.8 (10.9)				9.08	19.5	14.1	5.35	4.29	52.4	0.142

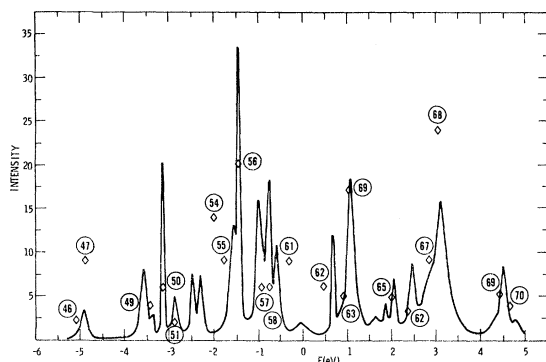


FIG. 7. Calculated and measured $2p-(3p)^2$ satellite spectra of Ar, resulting from the addition of the $L_{23}M_1-M_1(M_{23})^2$ spectrum to the solid spectrum in Fig. 6.

value. However, a comparison of Fig. 1 with the tabulation in Ref. 7 indicates the tabulated value is probably a misprint. Peaks 54 and 64 are not accounted for. But we have not yet included the $[2p][3s] \rightarrow [3s][3p]^2$ satellite structure. Table IV indicates that the strongest line in this spectrum is $[2p][3s]1a \rightarrow [3s][3p]^2D$. This line we identify as peak 64 at 194.66 eV. Using Mehlhorn's estimates² of the L_1 ionization energy, the $L_1-L_{23}M_1$ Auger electron energy, and the location of the $[3s][3p]^2D$ term, leads to a $[2p][3s]1a \rightarrow [3s][3p]^2D$ energy of 195.3. The difference 0.64 eV is slightly larger than the error (0.5 eV) assigned by Mehlhorn to the L_1 ionization energy. Doing the calculation for the $[2p][3s] \rightarrow [3s][3p]^2$ satellite spectrum leads to a calculated intensity value at 194.66 eV that is twice the measured value. Consequently, we reduced the populations of the $[2p][3s]$ terms by a factor of 2 (shown in parentheses in Table IV). The transition rate for $L_1-L_{23}M_1$ is then half the calculated value but twice Mehlhorn's estimate.² The result of adding both spectra is shown in Fig. 7. The results show reasonable agreement with experiment in shape, and agreement to within a factor of 2 in peak intensities. We have, thereby, accounted for peaks 46 to 78. Peaks 54 and 61 have no structure associated with them. If we shift level $2c$ by 0.25 eV (shown as the dashed line in Fig. 5), we can account for peak 61. This shift is in accord with Mehlhorn's assignment of 3D_2 . As a result, there is now a large peak at -2.25 eV which corresponds to the structure called peak 53 in Ref. 7. This is obscured by the principal spectrum peak 52. However, we have not identified peak 54.

As a consequence of this analysis of the $[2p]-[3p]^2$ satellite spectra, we obtain the $[2p]-[3s][3p]$ and $[2p]-[3s]^2$ satellite spectra with no free param-

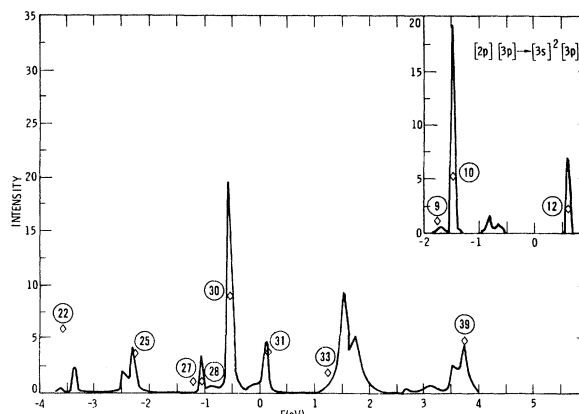


FIG. 8. Calculated and experimental $(2p)-(3s)(3p)$ satellite spectra. In the insert is shown the calculated and experimental $(2p)-(3s)^2$ satellite spectrum.

ters. The results are shown in Fig. 8. There is reasonable agreement in shape, and agreement to a factor of 2 in intensity.

IV. CONCLUSIONS

A comparison of the measured and calculated Ar principal $L_{23}MM$ spectra indicated that agreement was excellent if peaks assigned to the $L_{2,3}-M_1M_1$ transition and to satellites were reassigned to the $L_{23}-M_1M_{2,3}$ (1P) term. It was shown that the reassignment was consistent with the effect of configuration interaction on the position of the $M_1M_{2,3}$ (1P_1) term. Two doublets assigned to satellite structure were reassigned to the $L_{2,3}-M_1M_1$ transition. Examination of the $L_{2,3}-M_{2,3}M_{2,3}$ satellite structure supported Mehlhorn's assignment of the ten terms of the $[2p][3p]$ configuration in argon. All the peaks in Figs. 1 and 2 except peaks 1-8, 14-20, 42-44, and 79-82 were assigned either to the principal or the satellite spectra. The exceptions are all extremely small peaks. The satellite spectra indicate that, to within a factor of 2, σ_{2s}/σ_{2p} (the ratio of subshell electron ionization cross sections at 3 keV) is 0.05. A significant disagreement between theory and experiment is $I(L_1-L_{23}M_1)/I(L_1-L_{23}M_{23})$, the ratio of transition rates. The theoretical ratio is about unity, Mehlhorn² obtains a ratio of approximately 0.25. The experimental $L_1-L_{2,3}M_1$ peaks are superimposed on a large and rapidly rising background. Our analysis of the satellite spectra indicates a ratio of about 0.50. Mehlhorn's analysis indicates the calculated absolute $L_1-L_{23}M_{23}$ transition rate is correct. The difference between calculated and measured L_1 widths is then caused by the $L_1-L_{23}M_1$ transition rate. It has been observed¹⁶ that such a disagreement exists for the elements with $15 \leq Z \leq 21$, and is not limited to Ar.

A possible explanation for this is weak configuration interaction between $[2p][3s]^1P$ and $[2s][3p]^1P$, a large transition rate for $[2s] \rightarrow [2s][3p]$ (i.e., popping out an electron), and a destructive interference between the two transition rates. With this exception, calculation and experiment on the *MMM* Auger spectra of Ar are in good agreement. Finally, the analysis of Auger satellite spectra was

shown to be a useful technique in establishing the energy levels of atoms with multiple inner-shell vacancies.

ACKNOWLEDGMENT

I wish to thank Professor Bergmark of Uppsala University who kindly provided Figs. 1 and 2.

*This work supported by the U.S. Atomic Energy Commission.

¹E. J. McGuire, Phys. Rev. A **11**, 17 (1975).

²W. Mehlhorn, Z. Phys. **208**, 1 (1968).

³E. J. McGuire, Phys. Rev. A **3**, 1801 (1971).

⁴R. A. Rubenstein, Ph.D. thesis (University of Illinois, 1955) (unpublished).

⁵C. E. Moore, *Atomic Energy Levels*, Natl. Bur. Stand. Circ. No. 467 (U.S. GPO, Washington, D. C., 1949).

⁶E. J. McGuire, following paper, Phys. Rev. A **11**, 1889 (1975).

⁷L. O. Werme, T. Bergmark, and K. Siegbahn, Phys. Scr. **8**, 149 (1973).

⁸W. Mehlhorn and D. Stalherm, Z. Phys. **217**, 294 (1968).

⁹J. C. Slater, *Quantum Theory of Atomic Structure* (McGraw-Hill, New York, 1960).

¹⁰J. B. Mann, Los Alamos Scientific Report LASL-3690, 1967 (unpublished).

¹¹T. A. Carlson and C. W. Nestor, Jr., Phys. Rev. A **8**, 2887 (1973).

¹²E. J. McGuire, Phys. Rev. A **3**, 267 (1971).

¹³E. J. McGuire, J. Phys. (Paris) Suppl. **10**, **32**, C4-37 (1971).

¹⁴J. J. Vrakking and F. Meyer, Phys. Rev. A **9**, 1932 (1974).

¹⁵E. J. McGuire, Phys. Rev. A **11**, 10 (1975).

¹⁶E. J. McGuire, in *Atomic Inner Shell Processes*, edited by B. Crasemann (Academic, New York, 1975).